Journal of NUCLEAR SCIENCE and TECHNOLOGY, Vol. 37, No. 11, p. 949–958 (November 2000)

Status of JAERI Material Performance Database (JMPD) and Analysis of Irradiation Assisted Stress Corrosion Cracking (IASCC) Data

Yoshiyuki KAJI†, Yukio MIWA, Takashi TSUKADA,
Hirokazu TSUJI and Hajime NAKAJIMA

Department of Nuclear Energy System, Japan Atomic Energy Research Institute

(Received April 18, 2000), (Revised July 28, 2000)

A material performance database for nuclear applications, which was named the JAERI Material Performance Database (JMPD), has been developed since 1986 with a view to utilizing various kinds of characteristic data of nuclear materials efficiently. The data stored in the JMPD are mainly fatigue crack growth data on low alloy steels, creep data on superalloys, tensile data on aluminum alloys and stress corrosion cracking data (Slow Strain Rate Testing (SSRT), crack growth rate, *etc.*) on austenitic stainless steels.

Irradiation Assisted Stress Corrosion Cracking (IASCC) of austenitic stainless steels in high temperature water has been considered as a degradation phenomenon potential not only in light water reactors (LWRs) but in the rather common systems where the materials are exposed to radiation in the presence of water.

This paper describes the present status of the JMPD, which is partially available through the Internet. Furthermore, some trials for the utilization of the system focused on the issues relating to IASCC are mentioned. The effect of alloy composition, dissolved oxygen and neutron fluence on IASCC susceptibilities and SCC growth rate could be drawn.

KEYWORDS: material performance database, JMPD, irradiation, radiation effects, stress corrosion cracking, IASCC, IASCC susceptibility, SCC growth rate, alloy composition, dissolved oxygen, neutron fluence

I. Introduction

Recent remarkable improvements in the computational environment make it possible to extract sophisticated information easily and rapidly from complex materials data. Moreover, the World Wide Web (WWW), which is based on hypertext and is capable of moving a file from one document to another, is the predominant method to access the Internet. Many groups of researchers are now developing computerized material databases to have information on the general properties data for metals, alloys, composites, *etc.*[1)-5)]. Referring to the critical and technical assessment on the research and development in the field of nuclear technologies, the promotion of advanced materials research which could lead to technical breakthrough in many research fields is expected to be encouraged. In accordance with this new trend, a material performance database, which was named Japan Atomic Energy Research Institute Material Performance Database (JMPD)[6)-8)], has been developed since 1986 focusing on the storage of the data regarding research and development promoted by Japan Atomic Energy Research Institute (JAERI).

The in-core structural materials used in the light water reactors are exposed to high-flux neutron and gamma radiation in the high-temperature water environment. The radiation, stress and/or water cause various degradation phenomena on the structural materials. The irradiation-assisted stress corrosion cracking (IASCC) is known as one of such phenomena showing a synergistic effect of radiation, stress and water[9)]. The IASCC is considered to be one of the key issues for life assessment of the core internals of nuclear power plants, because the accumulation of radiation damage in the material is a primary cause of IASCC. The field experiences of IASCC failures indicate that the intergranular cracking (IG) occurs in austenitic stainless steels (SS), *e.g.*, type 304 SS. The threshold neutron fluence level has been reported to be around $5\times10^{24}n/m^2$ (E>1 MeV)[10)]. In both BWR and PWR, some in-core components such as bolts, sheath tubes, *etc.*, indicate the formation of IASCC.

The welded BWR core shrouds in relatively old plants have also experienced the cracking. In case of this failure, the fast neutron fluence level was somewhat lower than the threshold fluence level of IASCC, and the failure occurred at thermally sensitized part of the components. Therefore, the cracking of the core shroud has been considered as a thermally induced IGSCC. In Japan, the core shrouds of old plants were manufactured using type 304 SS and they will be replaced by new components made of type 316L SS that is more resistant to the thermally induced SCC. To confirm the effectiveness of the

* *Shirakata-Shirane, Tokai-mura, Naka-gun, Ibaraki 319-1195.*
† Corresponding author, Tel. +81-29-282-5386,
Fax. +81-29-282-5349, E-mail: kaji@popsvr.tokai.jaeri.go.jp

replacement material, it is worthwhile to compare the IASCC behavior of type 304 materials with that of 316 materials. The factors that cause the differences between both materials are to be studied.

This paper describes the present status of the JMPD, which is partially available through the Internet, along with some trials for the system utilization focusing on the issues relating to IASCC. Based on the knowledge derived from our post-irradiation examinations (PIEs), analysis of the IASCC data in JMPD was performed to confirm the dependence of IASCC susceptibility on alloy composition and test condition and the dependence of crack growth rate on environmental factors.

II. Outline of JMPD

Fundamental studies on structural materials have been performed at JAERI for practical applications to nuclear plants. For the evaluation of reliability and safety of structural materials, various material tests have been conducted. The JMPD was that for mechanical properties data such as fatigue crack growth, creep, tensile, low-cycle fatigue, slow strain rate testing (SSRT), *etc.*

Referring to more than ten materials databases which have been already developed in Japan and other countries[11)-13)], the data structure for metallic materials in the JMPD was originally determined in a three-level hierarchy. Six categories, *i.e.*, data source, material, specimen, test method and data reduction, test condition and test result, were classified into the primary level. Twenty-five tables were selected for the secondary level and more than 420 data items were prepared for the tertiary level.

The JMPD is implemented with Oracle, which is a relational database system on a workstation. A data entry supporting system with spreadsheet-type software is implemented on a personal computer and is connected to the JMPD by a middle software through Ethernet. The main feature of this system facilitates (a) to design the input sheet by extracting the data item from the data dictionary of the JMPD, (b) to enter the data by using the guide function. Users can access the Internet through their own computers in the WWW browser, retrieve the required data from JMPD and output the graph.

The data stored in the JMPD by the end of March 2000 are listed in **Fig. 1**, in which the data from more than 11,000 test pieces were prepared for evaluation. The data stored were checked through the author's review in order to prevent unexpected miss-input within the range of possibility. Only the data of the materials whose origins such as chemical compositions and heat treatment conditions as well as experimental methods were clear have been stored.

The JMPD was designed for effective utilization of material data especially for environmentally assisted degradation, *e.g.*, fatigue or SCC behavior in aqueous or gaseous environments. As for a part of IASCC database, about 300 data of post irradiation SSRT from our experimental work and 20 open published papers were input. The IASCC data consist of those of type 304 and 316 materials at irradiation temperatures between 333 and 573 K. The fast neutron fluences to the materials are in the range of from $1\times10^{22}n/m^2$ to $8\times10^{26}n/m^2$ (E>1 MeV). The IASCC susceptibilities of the materials had been examined by SSRT at around 573 K in high-temperature water containing dissolved oxygen concentration between 1 ppb and 32 ppm. Data analyses were performed with the knowledge on the factors controlling IASCC obtained by our results of the post irradiation SSRT[14)-16)].

As for the part of the SCC database, about 1,000 data of SCC growth rate from 21 published papers were input. The SCC growth rate data consist of those of thermally

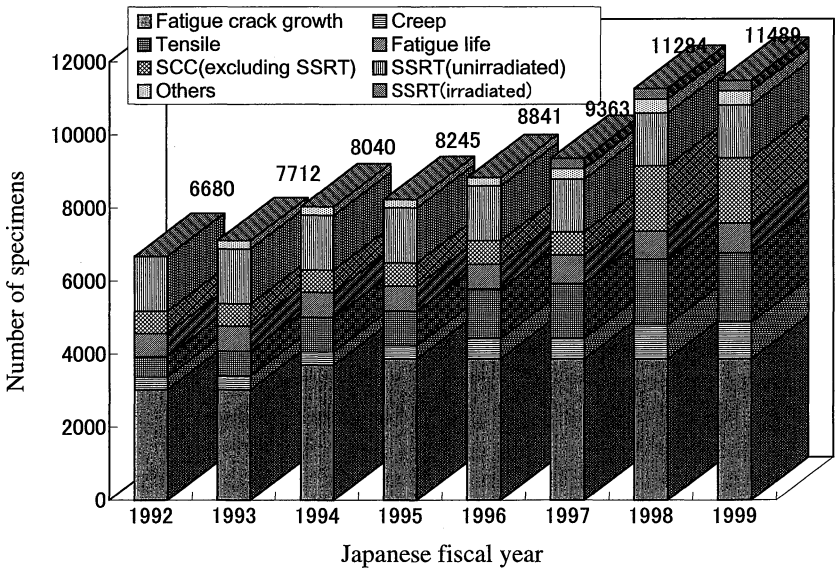

Fig. 1 Transition of the data stored in JMPD at the end of each fiscal year

sensitized type 304 and 316 alloys under constant load condition at 403–561 K in high temperature water containing various concentration levels of dissolved oxygen.

III. Post Irradiation Examinations

1. Materials and Irradiation

The chemical compositions of specimen materials are listed in **Table 1**. Two kinds of high-purity base alloys, HP304 and HP316, have similar concentrations of major alloying elements except for molybdenum. The other twelve alloys were doped with minor elements, *i.e.*, carbon, silicon, phosphorus, sulfur and titanium, into the base alloys to evaluate separately the effect of those elements on IASCC. The alloys were solution annealed and machined to round bar type specimens with the dimensions shown in **Fig. 2**. The neutron irradiation of the specimens was carried out in an irradiation capsule loaded into the Japan Research Reactor No. 3 Modified (JRR-3M), which is a 20MW pool type reactor, with a neutron fluence of $6.7\times10^{24} n/m^2$ (E>1 MeV) at 513 K.

2. Slow Strain Rate Testing (SSRT) in High Temperature Water

The SCC susceptibility of the irradiated specimens in high temperature water was evaluated by the SSRT method using a test apparatus installed in a hot cell at the Oarai Hot Laboratory of JAERI. It consists of a tensile test apparatus, an autoclave and a water circulation system as illustrated in **Fig. 3**. The SSRT experiments were carried out in high-temperature water at 573 K in 9.3 MPa and at an initial strain rate of $1.7\times10^{-7}\,s^{-1}$. The flow rate of water into the autoclave was 5 l/h. The dissolved oxygen (DO) concentration was controlled to the saturation level by water purification and make-up units in the water circulation system. The electrical conductivity of the inlet water to the autoclave was kept below 0.2 μS/cm.

3. SEM and TEM Analyses

After the SSRT tests, all specimens were examined by the scanning electron microscope (SEM) and the fractions of the SCC area on the fracture surfaces were evaluated as IASCC susceptibility.

The radiation induced segregation (RIS) of alloy elements at the grain boundaries may be the most impor-

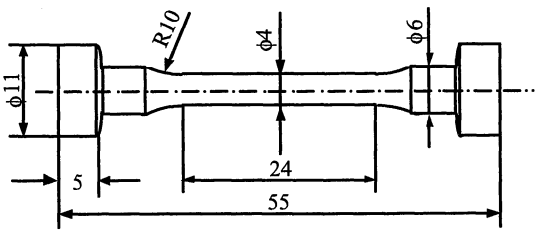

Fig. 2 SSRT specimen (unit: mm)

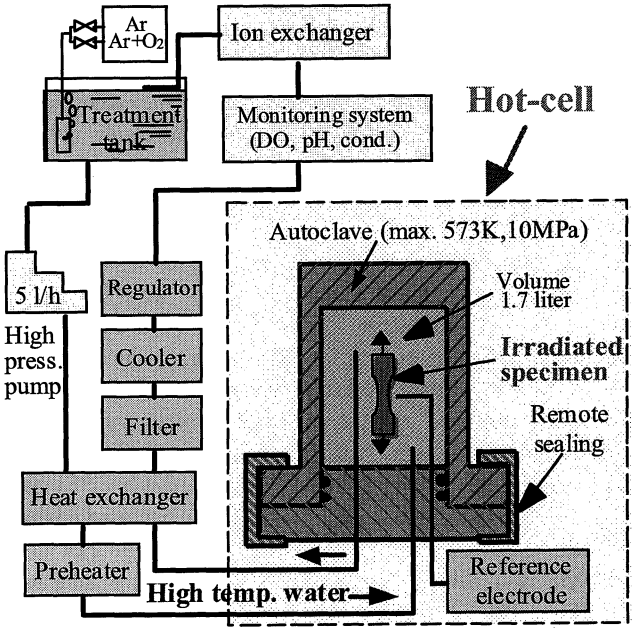

Fig. 3 SSRT test machine at hot laboratory

Table 1 Chemical compositions of model stainless steels (unit: wt%)

Alloy ID	C	Si	P	S	Mn	Cr	Ni	Mo	Ti	Fe
HP304	**0.003**	**0.01**	**0.001**	**0.001**	**1.36**	**18.17**	**12.27**	—	**0.01**	**Bal.**
HP304/Si	0.003	0.69	0.001	0.001	1.36	18.01	12.24	—	0.01	Bal.
HP304/P	0.006	0.03	0.017	0.001	1.40	18.60	12.56	—	0.01	Bal.
HP304/S	0.002	0.03	0.001	0.032	1.41	18.32	12.47	—	0.01	Bal.
HP304/C	0.098	0.03	0.001	0.002	1.39	18.30	12.50	—	0.01	Bal.
HP304/C/Ti	0.099	0.03	0.001	0.002	1.39	18.50	12.47	—	0.31	Bal.
HP304/All	0.107	0.72	0.019	0.036	1.41	18.66	12.68	—	0.29	Bal.
HP316	**0.004**	**0.02**	**0.001**	**0.001**	**1.40**	**17.21**	**13.50**	**2.50**	**0.01**	**Bal.**
HP316/C	0.061	0.03	0.001	0.001	1.40	17.28	13.50	2.49	0.01	Bal.
HP316/C/Ti	0.062	0.04	0.001	0.001	1.39	17.05	13.47	2.48	0.29	Bal.
HP316/C/Ti/Si	0.065	0.70	0.001	0.001	1.39	17.16	13.53	2.44	0.30	Bal.
HP316/C/Ti/P	0.061	0.05	0.019	0.002	1.40	16.95	13.53	2.48	0.29	Bal.
HP316/C/Ti/S	0.061	0.03	0.001	0.037	1.41	17.82	13.60	2.47	0.30	Bal.
HP316/All	0.063	0.76	0.018	0.037	1.42	17.32	13.56	2.43	0.30	Bal.

tant factor affecting IASCC. However, since the compositional profiles by RIS in the vicinity of grain boundaries are very narrow around 5 nm in width, the qualitative analyses of the profiles could not be made by conventional type transmission electron microscope (TEM). At JAERI then, the microstructural analyses of irradiated specimen were performed with a field emission gun type TEM to examine the radiation-induced microstructural and microchemical effects[17)(20)]. To reduce the detrimental effect of gamma radiation from irradiated TEM specimen on the compositional analysis using energy dispersive spectrometer (EDS), the specimen was miniatured to about 1/50 volume of conventional TEM specimens.

IV. Experimental Results of Post Irradiation SSRT

Some examples of engineering stress-strain curves during SSRTs are shown in **Fig. 4** for type 304 and 316 alloys[16)]. In Fig. 4(a), the results for HP304, HP304/C, HP316 and HP316/C are presented. The alloy HP316 doped with molybdenum showed a lower yield stress than that of HP304 alloys, but the maximum tensile stresses for both alloys were nearly the same. The addition of carbon into both HP304 and HP316 alloys caused a fairly large radiation hardening. The total elongation of the specimens doped with molybdenum was larger than those of HP304 and HP304/C alloys because the latter alloys failed by a large fraction of IGSCC (intergranular stress corrosion cracking) and TGSCC (transgranular stress corrosion cracking). Figure 4(b) shows the stress-strain curves for alloys doped with silicon and sulfur, where three alloys doped with molybdenum (HP316/C/Ti, HP316/C/Ti/Si and HP316/C/Ti/S) showed higher strength because carbon was added into those alloys in 0.06 wt% but not into the type 304 alloys. In each series of type 304 and 316 alloys, two alloys doped with silicon, *i.e.*, HP304/Si and HP316/C/Ti/Si, showed the largest total elongation. The total elongation for alloys doped with sulfur, HP304/S and HP316/C/Ti/S, was smaller than that for the other alloys. There is slight difference in the stress-strain curves in the alloys doped with carbon and titanium and with carbon, titanium and silicon for type 316 alloys.

In **Fig. 5**, the IASCC susceptibilities of the irradiated materials are summarized, where the ratios of the intergranular (IG) or transgranular (TG) cracking area to the whole fracture area are illustrated in terms of IASCC fractions[15)(16)]. It is known from field experience that the IASCC in power plants appears as IG cracking. Therefore, the comparison of the susceptibilities to IG type IASCC is more important in Fig. 5. In case of the SCC test by SSRT, the occurrence of TGSCC has frequently been reported, which is probably due to the severe loading condition in SSRT to maintain a constant strain rate.

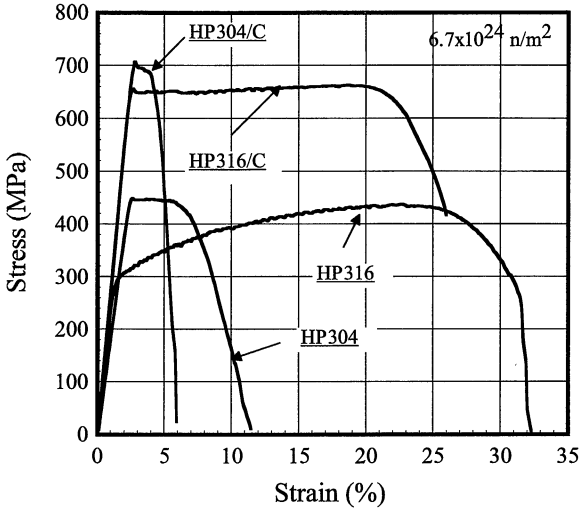

(a) Effect of Mo and C

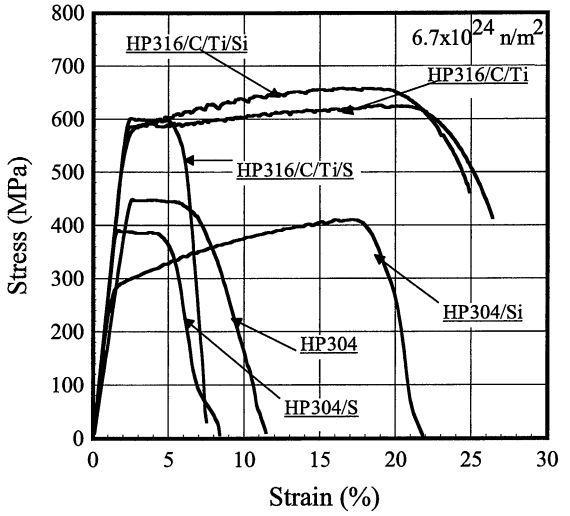

(b) Effect of S and Si

Fig. 4 Stress-strain behavior of irradiated specimen during SSRT in high temperature water at 573 K

The effects of addition of carbon, molybdenum and sulfur on IASCC behavior can be derived from Fig. 5. In a series of type 304 alloys, the effect of carbon addition can obviously be seen on fracture morphology. The dominant fracture mode of alloys without carbon addition was IGSCC. However, the addition of about 0.1 wt% carbon caused a change to TGSCC. Comparing HP304 with HP316, or HP304/C with HP316/C, we can conclude that the addition of molybdenum entirely suppresses the IASCC susceptibility. Only two alloys, *i.e.*, HP316/C/Ti/S and HP316/All, showed high susceptibilities to TGSCC and IGSCC of all the type 316 alloys, respectively. The elements commonly doped for both alloys are carbon, titanium and sulfur. In addition, the type 304 alloys doped with sulfur, *i.e.*, HP304/S, showed the highest susceptibility to IASCC at 513 K in pure water. It can be concluded that the sulfur addition of about 0.04 wt% is very injurious to IASCC. On the

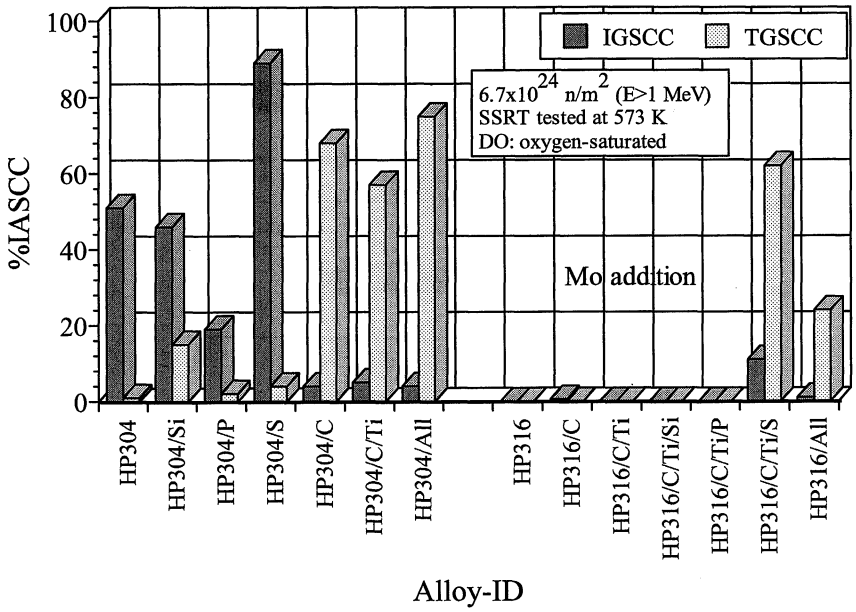

Fig. 5 IASCC susceptibility of the alloys irradiated up to $6.7\times10^{24}n/m^2$ at 513 K

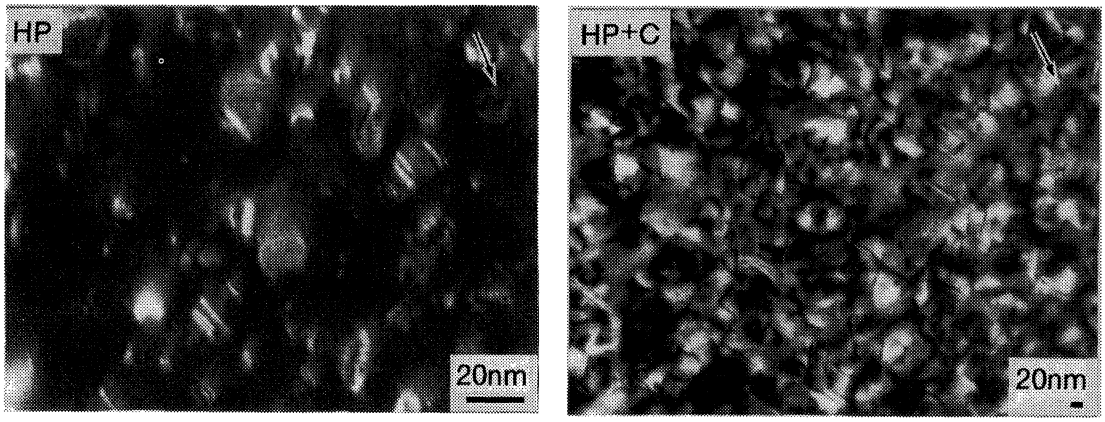

Photo. 1 Typical transmission electron micrographs of HP304 and HP304/C

other hand, the effect of silicon, phosphorus and titanium on IASCC susceptibility is not clear from Fig. 5, though it seems that an addition of phosphorus reduced the IASCC susceptibility as seen for HP304/P.

The HP304 alloys irradiated in JRR-3M were analyzed using FEG-TEM[17][20]. The major radiation defects were the Frank loops in all alloys. Additionally small defect clusters were observed as black dots. The weak-beam dark-field images of HP304 and HP304/C are shown in **Photo. 1**. In all alloys, the Frank loops and the small defect clusters composed the dominant microstructural features, while neither precipitates nor cavities were observed. The number density of small defect clusters in HP316 seemed to be lower than that in HP304. **Figure 6** shows the number density and average diameter of the Frank loops in these alloys. The number density and the average diameter in HP316 were smaller than those in HP304. Addition of molybdenum decreased the average diameter and the number density of the Frank loops, because the chemical compositions of these alloys were slightly different except for molybdenum content. By the addition of carbon in HP316, the number density of the Frank loops drastically increased and the average diameter decreased.

V. Analysis and Evaluation of Material Data through JMPD

1. SSRT Data Analysis

In **Fig. 7**, the IASCC susceptibility data compiled into the JMPD were plotted against fast neutron fluence (E>1 MeV). Though the percent IG cracking in the SSRT is a variable parameter, the susceptibility evaluation was made in terms of the IG cracking area in the SSRT for the common indicator in these database analyses. The data was scattered over a wide range of susceptibility against the neutron fluence. Since the dissolved oxygen (DO) content in high-temperature water is an es-

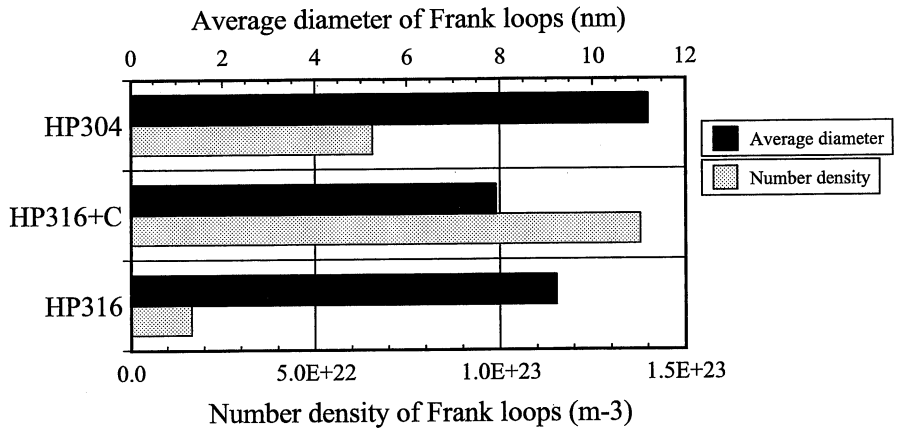

Fig. 6 Number density and average diameter of Frank loops

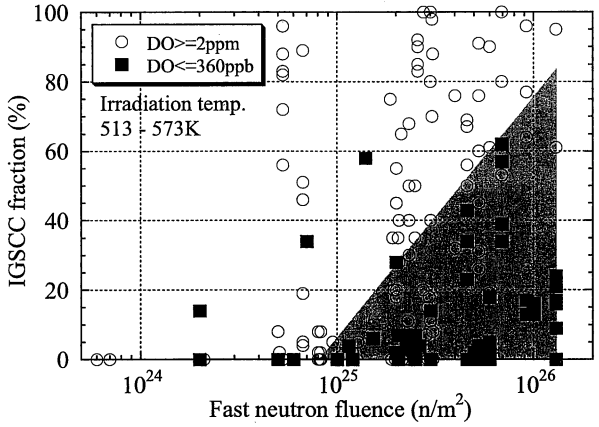

Fig. 7 Effect of dissolved oxygen (DO) on IASCC susceptibility of SSRT database in JMPD (all data)

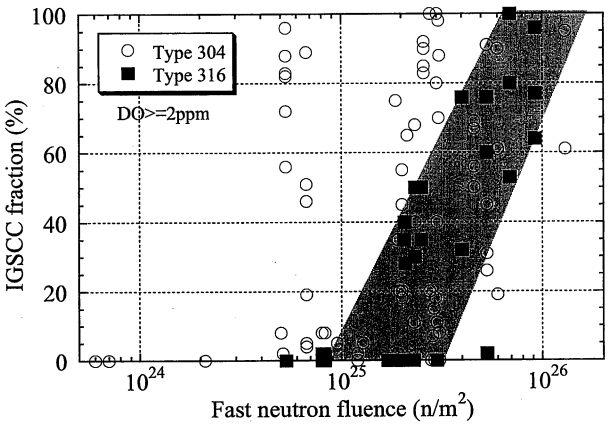

Fig. 8 Effect of molybdenum addition on IASCC susceptibility

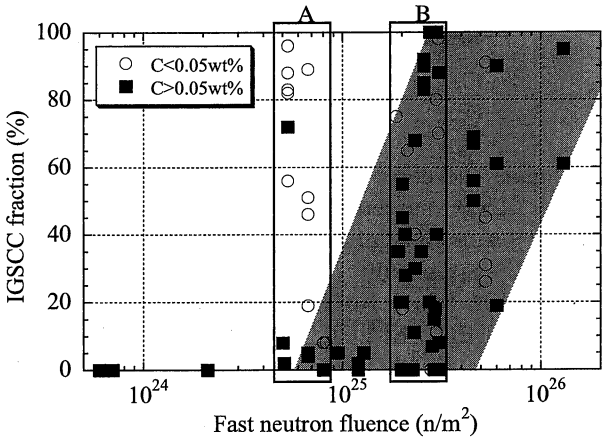

Fig. 9 Effect of carbon content on IASCC susceptibility

sential factor for SCC phenomena, all data are classified into two groups by levels of DO content during SSRT in Fig. 7. There is a tendency that the percent IG cracking of alloys tested in lower DO environment is smaller. According to the results of the post irradiation SSRT, the addition of molybdenum to 304 SS caused a drastic suppression of IASCC[14]. In **Fig. 8**, therefore, the data from the higher DO environment are plotted separately for type 304 and 316 alloys to confirm this effect. As seen there, at lower fluence levels around $1\times10^{25}n/m^2$, the type 316 alloys show smaller susceptibility compared with the type 304 alloys. This tendency may be due to the molybdenum addition. However, at higher fluence levels, the susceptibilities of the type 316 alloys are increasing with increasing fluence causing smaller difference in the susceptibilities of the type 304 and 316 alloys at the neutron fluence. In **Fig. 9**, the data from the type 304 alloys in Fig. 8 are plotted into two ranges of bulk carbon content. Some data discussed here are for uncontrolled 304 SS alloys. Namely, not only carbon but also nickel, nitrogen, *etc.*, are the variables. Tsukada *et al.* had found that the addition of carbon appeared to promote the TGSCC and suppress the IGSCC by means of post-irradiation SSRT experiments of type 304 alloys with the addition of carbon[14]-[16]. Therefore, by combination of the PIEs and database analysis, the effect of the carbon addition to suppress IASCC could appear at lower fluence levels around 5×10^{24}–$9\times10^{24}n/m^2$ (E>1 MeV). However, at higher fluence levels around 2×10^{25}–$3\times10^{25}n/m^2$, the effect seems to be lost as seen

in two boxes shown in Fig. 9.

Comparing the IASCC behavior of the materials, we derived the effect of carbon and molybdenum on IASCC susceptibility and its fracture morphology. In the case of SCC of unirradiated thermally sensitized stainless steels, the effect of carbon on IGSCC had been recognized distinctly, because thermal sensitization primarily depends on precipitation of Cr-carbide and a consequent chromium depletion at grain boundaries (GBs). However, in the case of IASCC, the effect of carbon had not been determined clearly. In this study, however, it was shown that the effect of carbon addition was significantly large at a lower neutron fluence level around "threshold" fluence of IASCC. The addition of carbon caused suppression of the IG type IASCC. This effect can be discussed from two viewpoints that are relating to the mechanical property and microchemistry of irradiated alloys.

In **Fig. 10**, the data of mechanical properties of tensile strength and elongation to fracture compiled in the JMPD are plotted against fast neutron fluence (E>1 MeV). All data are classified into two groups by bulk carbon content. The alloys with high carbon content tend to show higher tensile strength and lower elongation to fracture compared with those with low carbon content. That is, the addition of carbon enhances the radiation hardening. Tsukada *et al.* had found that the addition of carbon enhanced the radiation hardening[15][16] and it increased the number density of the Frank loops[17]. It may be suggested that the radiation hardening of alloy matrix suppresses consequently the plastic deformation or slip deformation near GBs that is needed for crack propagation through the slip dissolution mechanism[21]-[23] at lower fluence levels. Moreover, the addition of carbon is expected to reduce the chromium depletion at GBs, because it increases the number density of the Frank loops which serve as trapping sites for point defects. Therefore, the flow of point defects and the subsequent radiation induced depletion of chromium at GBs will be reduced. These two effects of carbon addition may suppress the susceptibility to IG type IASCC. Analysis of the IASCC database in JMPD revealed that the above-mentioned effect of carbon addition became increasingly indistinct at higher fluence levels of $10^{25}n/m^2$ (E>1 MeV) as seen in Fig. 9. It could be supposed that at these fluence levels the effect of carbon addition becomes relatively small, because the radiation hardening and the chromium depletion due to the radiation-induced segregation (RIS) nearly saturate regardless of carbon addition. It is likely that other factors are affecting the IASCC behavior which are more essential at higher fluence levels. As for these other factors, such as the dislocation channeling, the decreasing of the grain boundary binding energy by the hydrogen, the stability of the austenitic phase, *etc.*, are related with the IASCC initiation. Therefore, it is important to investigate the mechanisms considering not only the change of the composition in the grain boundary, the increasing of the strength, but also the local strength change such as the dislocation channeling and the interaction with the corrosion environment.

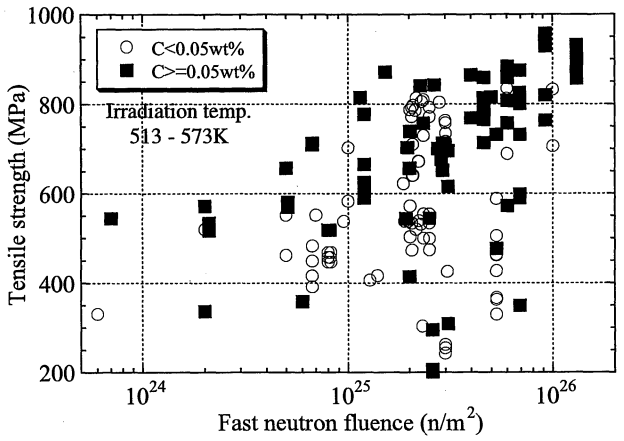

(a) Tensile strength

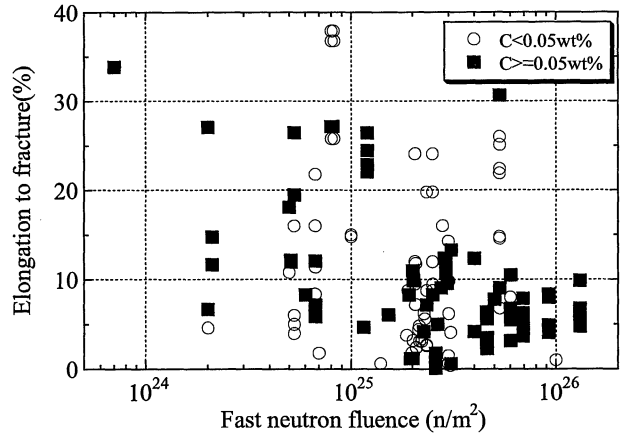

(b) Elongation to fracture

Fig. 10 Effect of carbon content on mechanical properties

The importance of molybdenum on IASCC has been suggested[18][19]. We clarified this by means of post-irradiation SSRT experiments of the alloy added with molybdenum[14]-[16]. The effect of molybdenum addition to suppress IASCC was remarkably large, though it gradually decreased at higher fluence levels above about $2\times10^{25}n/m^2$ (E>1 MeV) according to our database analysis as seen in Fig. 8. The tensile strength and the elongation to fracture are plotted separately against fast neutron fluence for type 304 and 316 alloys in **Fig. 11** to confirm the effect of molybdenum. As seen in Fig. 11, however, the addition of molybdenum has no marked influence on mechanical properties after irradiation, though type 316 alloys show a little lower tensile strength and higher elongation to fracture compared with those of type 304 alloys. It is obvious that in the case of SCC, due to thermal sensitization, the addition of molybdenum is very effective to mitigate SCC. This is considered to be true because molybdenum stabilizes a passive film formed on stainless steels. A similar mech-

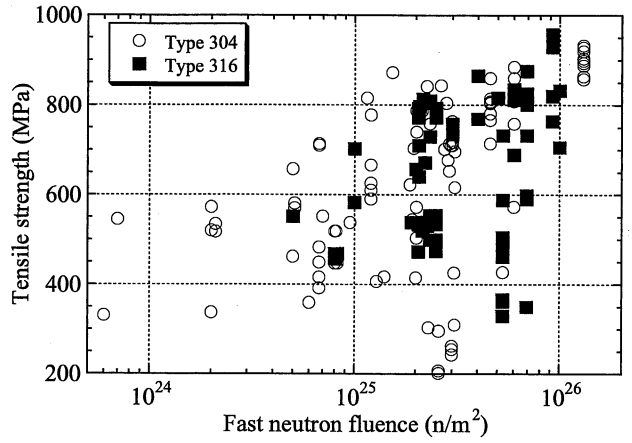

(a) Tensile strength

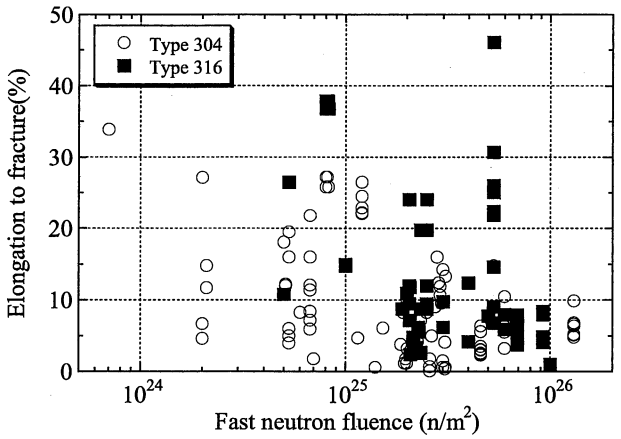

(b) Elongation to fracture

Fig. 11 Effect of molybdenum addition on mechanical properties

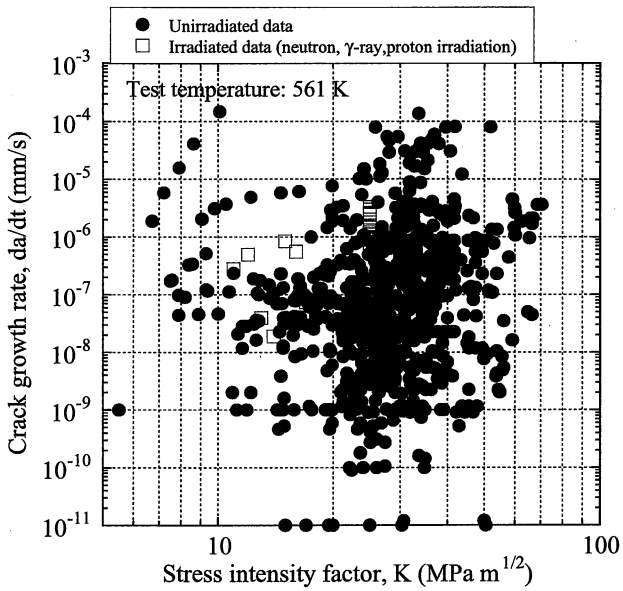

Fig. 12 SCC growth rate database in JMPD (all data)

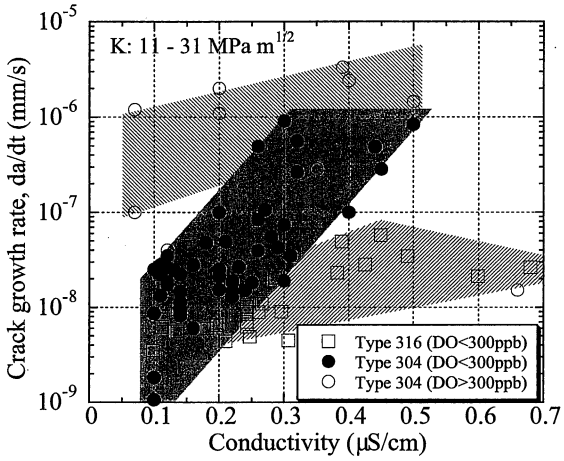

Fig. 13 Relationship between da/dt and electrical conductivity

anism can be suggested for IASCC, because the addition of molybdenum decreased the number density of the Frank loops as Miwa *et al.* reported[20]. The reduction of RIS at GBs is not expected to occur.

In BWRs, the fast neutron fluence on core shroud at the end-of-life is estimated to be about $2\times10^{25}n/m^2$. The present results from post irradiation SSRT and from database analysis support the effectiveness of replacement of type 304 by type 316L alloys. At lower neutron fluence levels, the reduction of carbon content may cause an enhancement of IASCC of type 304 alloys.

2. Crack Growth Data Analysis

The data analysis was performed based on the knowledge about the factors controlling SCC. In **Fig. 12**, all the data of SCC growth rate da/dt at 561 K for unirradiated and irradiated type 304 and 316 alloys compiled into the JMPD from the literature are plotted against stress intensity factor, K. The data including the irradiated data are seen to scatter over a wide range of crack growth rate making it difficult to deduce the effect of radiation on da/dt. Therefore, the data analysis was hereafter carried out for sensitized type 304 and 316 alloys including the irradiated data. Suzuki *et al.*[24] reported that the crack growth rate of SCC was affected by specimen thickness. They observed that the thicker specimens showed lower crack growth rates for sensitized 304 SS. Though the size effect of the SCC growth rate is one of the key factors of the SCC growth behavior, we cannot extract the size effect on SCC growth rate for the specimens in this database analysis, because of inadequate data on SCC growth for 1/4TCT specimens. Most of the SCC growth data are for 1TCT specimens in JMPD.

Figure 13 shows the relationship between da/dt and electrical conductivity of the water. The data are classified into three groups by the level of dissolved oxygen and alloy type. The SCC growth rate da/dt in lower DO environment is found to be lower than that in higher DO environment for type 304 alloys. The rate for type 316 alloys is lower than that for type 304 alloys under the

same DO condition.

Since the DO content in high temperature water is an essential factor for SCC growth rate, all data are classified into three groups by the level of DO content and alloy type on *da/dt-K* relationship in **Fig. 14**. A tendency observed is that the SCC growth rate of both type 304 and 316 alloys tested in lower DO environment is lower than that in higher DO environment in Fig. 14. It is difficult to deduce any relation between type 304 and 316 alloys regarding *da/dt-K* relationship under lower DO condition, because the data are scattered over a wide range of *da/dt* through the *K* for type 304 alloys.

In **Fig. 15**, therefore, the rates from type 304 alloys are plotted separately to confirm the effect of dissolved hydrogen (DH) on the *da/dt-K* relationship. The range of DH is from 50 to 500 ppb for BWR condition in Fig. 15. As shown in Fig. 15, the rates in lower DO and DH environments show lower values compared with those under normal DO environments. This can be attributed to the DH addition.

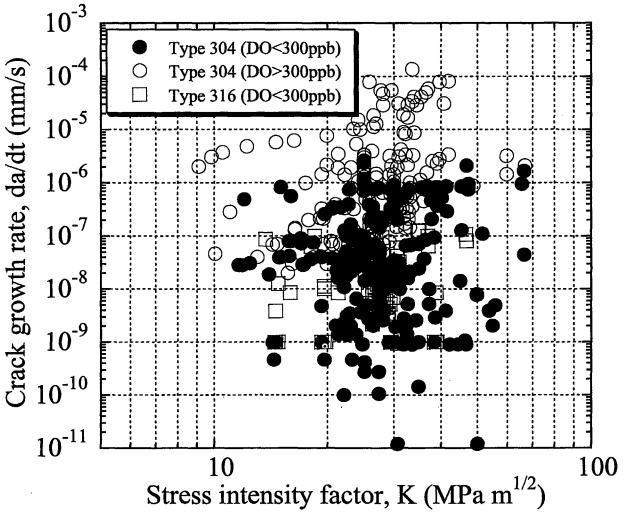

Fig. 14 Effect of dissolved oxygen (DO) on *da/dt-K* relationship

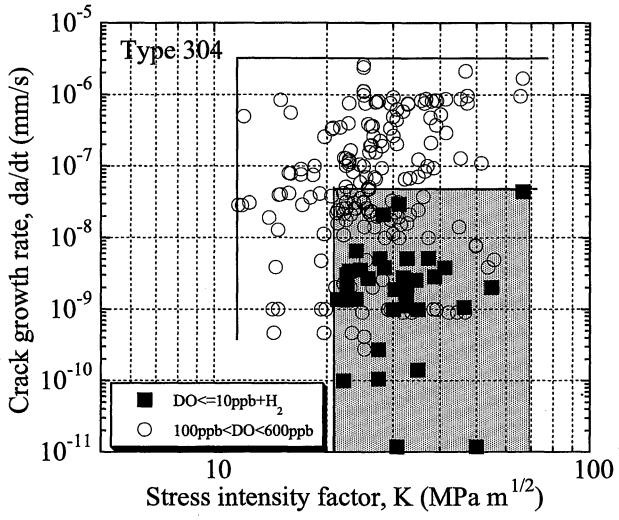

Fig. 15 Effect of hydrogen addition on *da/dt-K* relationship

Regarding utilization of the database, it is important to confirm the heat treatment conditions and the detailed experimental conditions *etc.*, of the materials, before narrowing the data and making a comparison with the experimental data. Otherwise it may well be that users will judge negatively the new experimental results.

The future subjects would be those to get and store sufficient reliable data for IASCC susceptibility and SCC crack growth for irradiated type 304 and 316 alloys under sufficiently controlled high temperature water condition in the JMPD, because it is important to resolve clearly the mechanism of IASCC by using both PIEs results including microstructural analyses and reliable database.

VI. Conclusions

The Japan Atomic Energy Research Institute Material Performance Databse (JMPD) has been developed with attention paid to substantial user-friendliness of the system. The present status of the system and some trials of application utilization of the system on the issues relating to irradiation-assisted stress corrosion cracking (IASCC) are described. From the analysis of the IASCC data in JMPD based on the knowledge derived from our results of the post-irradiation examinations (PIEs), the following conclusions are obtained:

-Slow strain rate cracking (SSRT) data analysis

(1) By means of the combination of the post irradiation SSRT and database analysis, the dependence of IASCC susceptibilities on alloy composition, neutron fluence and dissolved oxygen level could be drawn.

-SCC growth rate data analysis

(2) Crack growth rate in high temperature water containing lower levels of dissolved oxygen (DO) and electrical conductivity is low under the same stress intensity factor.

(3) Addition of hydrogen to normal DO environments remarkably suppresses the crack growth rate.

Acknowledgement

The authors are grateful to Mr. T. Sakino and Ms. T. Yoshikawa of Japan Atomic Energy Research Institute for their assistance in the data search procedure from the Japan Atomic Energy Research Institute Material Performance Database.

—References—

(1) Doyama, M., Suzuki, T., Kihara, J., Yamamoto, R.: "*Computer Aided Innovation of New Materials*", Elsevier Sci. Publ., Netherlands, (1991).

(2) Doyama, M., Kihara, J., Tanaka, M., Yamamoto, R.: "*Computer Aided Innovation of New Materials* (II)", Elsevier Sci. Publ., Netherlands, (1993).

(3) Glazman, J. S., Rumble, J. R., ed.: *ASTM-STP* 1017, (1989).

(4) Barry, T., Reynard, K., ed.: *ASTM-STP* 1140, (1992).

(5) Nishijima, S., Iwata, S., ed.: *ASTM-STP* 1311, (1997).

(6) Yokoyama, N., Tsukada, T., Nakajima, H.: *JAERI-M*90-237, (1987), [in Japanese].
(7) Tsuji, H., Yokoyama, N., Tsukada, T., Nakajima, H.: *J. Nucl. Sci. Technol.*, **30**, 1234 (1993).
(8) Yokoyama, N., Tsuji, H., Tsukada, T., Shindo, M.: *ASTM STP* 1311, p. 261 (1997).
(9) Scott, P.: *J. Nucl. Mater.*, **211**, 101 (1994).
(10) Andresen, P. L., Ford, F. P., Murphy, S. M., Perks, J. M.: *Proc. 4th Int. Symp. on Environmental Degradation of Materials in Nuclear Power Systems—Water Reactors*, Jekyll Island, GA, NACE, p. 1 (1990).
(11) Rumble, J., Northrup, C., Westbrook, J., Grattidge, W., McCarthy, J.: Materials Information for Science and Technology (MIST), Project Overview, US Department of Commerce, (1986).
(12) Mindlin, H., Rungta, R., Koehl, K., Gubiotti, R.: *EPRI NP*-4485, (1986).
(13) Buchmayr, B., Krockel, H.: High Temperature Materials Databank (HTM-DBC), Comm. of the European Communities, Joint Res. Center, (1988).
(14) Tsukada, T., Miwa, Y., Tsuji, H., Mimura, H., Goto, I., Hoshiya, T., Nakajima, H.: *Proc. 7th Int. Conf. on Nuclear Engineering (ICONE-7)*, L4-3, (1999).
(15) Tsukada, T., Miwa, Y., Nakajima, H.: *Proc. 7th Int. Symp. on Environmental Degradation of Materials in Nuclear Power Systems—Water Reactors*, Breckenridge, CO, NACE, p. 1009 (1995).
(16) Tsukada, T., Miwa, Y., Nakajima, H., Kondo, T.: *Proc. 8th Int. Symp. on Environmental Degradation of Materials in Nuclear Power Systems—Water Reactors*, Amelia Island, FL, ANS, p. 795 (1997).
(17) Miwa, Y., Tsukada, T., Jitsukawa, S., Kita, S., Hamada, S., Matsui, Y., Shindo, M.: *J. Nucl. Mater.*, **233–237**, 1393 (1996).
(18) Jenssen, A., Ljungberg, L. G.: *CORROSION/96*, Paper No. 101, (1996).
(19) Kasahara, S.: *Proc. 6th Int. Symp. on Environmental Degradation of Materials in Nuclear Power Systems—Water Reactors*, San Diego, CA, TMS, p. 615 (1994).
(20) Miwa, Y., Tsukada, T., Tsuji, H., Nakajima, H.: *J. Nucl. Mater.*, **271&272**, 316 (1999).
(21) Andresen, P. L., Ford, F. P.: *Mater. Sci. Eng.*, **A103**, 167 (1988).
(22) Ford, F. P., Taylor, D. E., Andresen, P. L., Ballinger, R. G.: EPRI Contract RP2006-6, *Rep. NP*5064*M*, (1987).
(23) Ford, F. P., Andresen, P. L.: *Proc. 3rd Int. Symp. on Environmental Degradation of Materials in Nuclear Power Systems*, Traverse City, Michigan, p. 789 (1987).
(24) Suzuki, S., Itoh, W.: *Proc. 76th JSME Annu. Meeting*, Sendai, Japan, Vol. 1, p. 145 (1998).